Neutrino signal predictions from multi-dimensional core-collapse supernova models

Ko NAKAMURA (Fukuoka Univ., e-mail: *nakamurako@fukuoka-u.ac.jp*),
T. Takiwaki (NAOJ), J. Matsumoto (Keio Univ.), S. Horiuchi (Virginia Tech.), K. Kotake (Fukuoka Univ.)

Abstract

Systematic studies of core-collapse supernovae have been conducted based on hundreds of one-dimensional artificial models (O'Connor & Ott 2011,2013; Ugliano et al. 2013, Ertl et al. 2015) and two-dimensional self-consistent simulations (Nakamura et al. 2015;2019, Burrows & Vartanyan 2020). We have performed three-dimensional core-collapse simulations for 16 progenitor models covering ZAMS mass between 9 and 24 solar masses. Our CCSN models show a wide variety of shock evolution, explosion energy, as well as multi-messenger signals including neutrinos. We present the dependence of the neutrino properties on the progenitor structure.

Numerical set-ups

- Code: 3DnSNE_MHD (*Takiwaki+'16,'18; Matsumoto+'20*).
- B-field: dipole formula with $B_0 = 10^{10}$ [G] and cutoff $R = 10^3$ km.
- Space domain: $0 \leqq R \leqq 10^4$ km, $0 \leqq \theta \leqq \pi$, $0 \leqq \phi \leqq 2\pi$
  with 600(r) x 64(θ) x 128(ϕ) grids.
- Progenitor: 9 - 24 $M_\odot$ (16 models),
  solar metallicity, non-rotating (*Sukhbold+'16*)

3D MHD simulations have been conducted from gravitational collapse to core bounce, shock stall and revival, up to 500ms after the bounce.

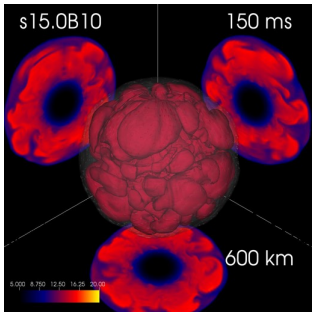

Figure 1. Entropy distribution for 15 $M_\odot$ model at 150ms after bounce. Strong convective motions, stimulated by neutrino heating, are visible behind the shock. The spatial scale (600km) is the size of the visualization box.

Shock evolution

All models present shock stalling at $R \sim 150$km, then successful shock expansion at $t < 300$ ms with the aid of neutrino heating. The neutrino heating efficiency is enhanced by multi-dimensional flow motions such as convection. One key aspect is a density drop at the chemical discontinuity layer involved in some models, which results in a sudden decrease of mass accretion and ram pressure onto the shock surface. It stimulates the stalling shock and leads to shock expansion. For the models with a small density drop, it takes a longer time to shock revival.

Figure 2. Time evolution of mass accretion rate estimated at $R = 500$ km. The accretion rate suddenly decreases when a density discontinuity falls into the central region. The density drops typically correspond to the interface between Si and O-rich layers. Note that the accretion rate also decreases when the shock turns to expand and suppress accretion flows.

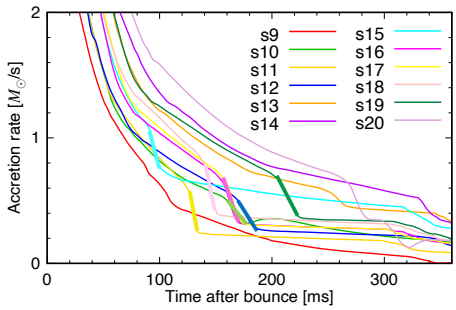

Figure 3. Time evolution of angle-averaged shock radius. The shock of all models once stalls at $R \sim 150$ km. Some of the models show a jump when the density drop falls onto the shock surface.

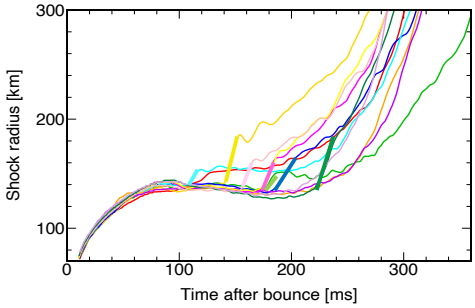

Neutrinos

A huge number of neutrino detection events from a Galactic CCSN are expected. Here we estimate the event numbers under the assumptions that the CCSN appears at the Galactic center (D=10kpc) and the detector is Super-Kamiokande (SK).
The detection number is almost identical in the very early phase (< 30 ms). But it soon become distinguishable reflecting the different accretion history. The sudden drops at ~150 ms in the models s11 and s18 are marginally detectable.

Figure 4. Expected neutrino detection events by SK, assuming the distance to the SN $D = 10$ kpc. The error bands are root-N Poisson. The declines at ~150 ms are caused by the decrease of the accretion rates seen in Fig. 2. No oscillation is considered here.

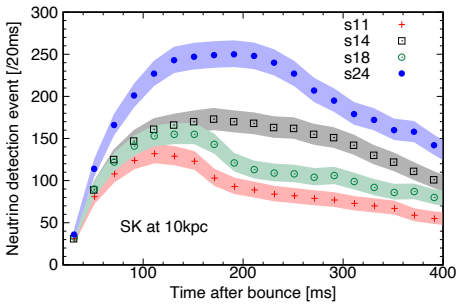

Figure 5. Cumulative detection numbers N(<t) under the same assumptions in Fig. 4, as a function of the compactness ξ_M. Shown are N(<200ms) with $\xi_{1.75}$ (filled circles) and N(<500ms) with $\xi_{2.5}$ (open circles). The latter shows a large dispersion since $\xi_{2.5}$ cannot characterize the drops in Figures 2&4. Note that the horizontal axis is arbitrary calibrated.

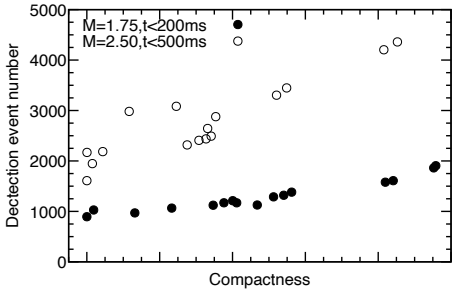

The highly non-spherical matter motions as shown in Figure 1 make anisotropic neutrino radiation. 10%-level deviations of the neutrino flux are commonly observed in our models. Figure 6 shows the deviation of the electron anti-neutrino flux from its angle average. This anisotropic distribution is maintained after shock revival and affects neutrino observations discussed above.

Figure 6. Mollweide-like plot showing the deviation of the luminosity of electron anti-neutrino from its angle average. Shown is the s14 model at 500ms after bounce as an example.

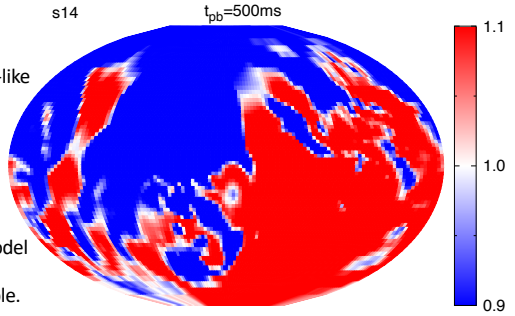

References

Takiwaki+'16, MNRAS Letters, 461, L112; Takiwaki+'18, MNRAS Letters, 475, L91; Matsumoto+'20, MNRAS, 499, 4174; Sukhbold+'16, ApJ, 821, 38